





Disrupted basal ganglia–thalamocortical loops in focal to bilateral tonic-clonic seizures

 Xiaosong He,¹  Ganne Chaitanya,² Burcu Asma,²  Lorenzo Caciagli,^{1,3}
 Danielle S. Bassett,^{1,4,5,6,7,8,*} Joseph I. Tracy^{2,*} and Michael R. Sperling^{2,*}

*These authors contributed equally to this work.

Focal to bilateral tonic-clonic seizures are associated with lower quality of life, higher risk of seizure-related injuries, increased chance of sudden unexpected death, and unfavourable treatment outcomes. Achieving greater understanding of their underlying circuitry offers better opportunity to control these seizures. Towards this goal, we provide a network science perspective of the interactive pathways among basal ganglia, thalamus and cortex, to explore the imprinting of secondary seizure generalization on the mesoscale brain network in temporal lobe epilepsy. Specifically, we parameterized the functional organization of both the thalamocortical network and the basal ganglia–thalamus network with resting state functional MRI in three groups of patients with different focal to bilateral tonic-clonic seizure histories. Using the participation coefficient to describe the pattern of thalamocortical connections among different cortical networks, we showed that, compared to patients with no previous history, those with positive histories of focal to bilateral tonic-clonic seizures, including both remote (none for >1 year) and current (within the past year) histories, presented more uniform distribution patterns of thalamocortical connections in the ipsilateral medial-dorsal thalamic nuclei. As a sign of greater thalamus-mediated cortico-cortical communication, this result comports with greater susceptibility to secondary seizure generalization from the epileptogenic temporal lobe to broader brain networks in these patients. Using interregional integration to characterize the functional interaction between basal ganglia and thalamus, we demonstrated that patients with current history presented increased interaction between putamen and globus pallidus internus, and decreased interaction between the latter and the thalamus, compared to the other two patient groups. Importantly, through a series of ‘disconnection’ simulations, we showed that these changes in interactive profiles of the basal ganglia–thalamus network in the current history group mainly depended upon the direct but not the indirect basal ganglia pathway. It is intuitively plausible that such disruption in the striatum-modulated tonic inhibition of the thalamus from the globus pallidus internus could lead to an under-suppressed thalamus, which in turn may account for their greater vulnerability to secondary seizure generalization. Collectively, these findings suggest that the broken balance between basal ganglia inhibition and thalamus synchronization can inform the presence and effective control of focal to bilateral tonic-clonic seizures. The mechanistic underpinnings we uncover may shed light on the development of new treatment strategies for patients with temporal lobe epilepsy.

- 1 Department of Bioengineering, University of Pennsylvania, Philadelphia, Pennsylvania, USA
- 2 Department of Neurology, Thomas Jefferson University, Philadelphia, Pennsylvania, USA
- 3 Department of Clinical and Experimental Epilepsy, UCL Queen Square Institute of Neurology, London, UK
- 4 Department of Physics and Astronomy, University of Pennsylvania, Philadelphia, Pennsylvania, USA
- 5 Department of Electrical and Systems Engineering, University of Pennsylvania, Philadelphia, Pennsylvania, USA
- 6 Department of Neurology, University of Pennsylvania, Philadelphia, Pennsylvania, USA
- 7 Department of Psychiatry, University of Pennsylvania, Philadelphia, Pennsylvania, USA
- 8 Santa Fe Institute, Santa Fe, New Mexico, USA

Received April 24, 2019. Revised August 16, 2019. Accepted September 24, 2019

© The Author(s) (2019). Published by Oxford University Press on behalf of the Guarantors of Brain. All rights reserved.

For permissions, please email: journals.permissions@oup.com

Correspondence to: Danielle S. Bassett, PhD
 J. Peter Skirkanich Professor of Bioengineering
 Departments of Bioengineering, Physics and Astronomy, Electrical and Systems Engineering,
 Neurology, and Psychiatry
 University of Pennsylvania
 210 S. 33rd Street, 240 Skirkanich Hall
 Philadelphia, PA 19104-6321, USA
 E-mail: dsb@seas.upenn.edu

Keywords: focal to bilateral tonic-clonic seizures; thalamus; basal ganglia; network neuroscience; resting state functional connectivity

Abbreviations: FBTCS = focal to bilateral tonic-clonic seizures; FIAS = focal impaired awareness seizures; GPe/i = globus pallidus externus/internus; rsfMRI = resting state functional MRI; SN = substantia nigra; STN = subthalamic nucleus; TLE = temporal lobe epilepsy

Introduction

Over 70% of patients with focal epilepsies can occasionally experience focal to bilateral tonic-clonic seizures (FBTCS) (Forsgren *et al.*, 1996). The prevalence of FBTCS is associated with lower quality of life (Yoo *et al.*, 2014), higher risk of seizure-related injuries (Lawn *et al.*, 2004) and SUDEP (sudden unexpected death in epilepsy) (Walczak *et al.*, 2001; Harden *et al.*, 2017), as well as unfavourable treatment outcomes (Bone *et al.*, 2012; Keller *et al.*, 2015). Accordingly, control of FBTCS is an important objective, particularly for patients with drug-resistant focal epilepsies, such as temporal lobe epilepsy (TLE). Why some patients suffer from uncontrolled FBTCS and others do not remains a mystery, and it is desirable to learn more about them and develop new treatment strategies.

Despite the earlier nomenclature ‘secondarily generalized tonic-clonic seizures’, FBTCS are not truly generalized, but instead selective, affecting specific brain regions most intensely (Blumenfeld *et al.*, 2003; Holmes *et al.*, 2004; Schindler *et al.*, 2007). In particular, accumulating evidence has underscored the critical role of the thalamus and its interacting circuits during FBTCS. As an integrative hub in the brain (Hwang *et al.*, 2017), the thalamus projects distributed reciprocal connections to the entire cerebral cortex (Jones, 2007) and mediates communication between different brain networks (Sherman and Guillery, 2013). In the context of FBTCS, the thalamus may act as an extension of the epileptogenic network (Guye *et al.*, 2006), supporting the propagation of ictal activity to widespread cortical networks (Castro-Alamancos, 1999) by synchronizing abnormal cortical–subcortical electrical discharges (Blumenfeld, 2002; Norden and Blumenfeld, 2002). For example, thalamic hyperactivity has been observed during FBTCS (Hamandi *et al.*, 2006; Blumenfeld *et al.*, 2009). Compared to patients with focal seizures only, patients with additional FBTCS present extra thalamic atrophy (Yang *et al.*, 2017) and disrupted thalamocortical connections both structurally (Keller *et al.*, 2015; Chen *et al.*, 2019) and functionally (He *et al.*, 2015; Peng and Hsin, 2017).

As a ‘braking system’ between the cortex and thalamus (Vuong and Devergnas, 2018), the basal ganglia appear to

be involved in FBTCS as well. The basal ganglia are a complex group of nuclei, including the striatum (putamen, caudate, and ventral striatum), globus pallidus (externus, GPe, and internus, GPi), subthalamic nucleus (STN), and substantia nigra (SN) (Wichmann and DeLong, 2012). The basal ganglia act in a topographically segregated manner interacting with thalamus and cortex, constituting several parallel circuits including the direct (cortex–striatum–GPi–thalamus–cortex) and indirect (cortex–striatum–GPe–STN–GPi–thalamus–cortex) pathways (Alexander *et al.*, 1986, 1990; Smith *et al.*, 1998). While the basal ganglia are also hyperactive during FBTCS (Blumenfeld *et al.*, 2009), and patients with FBTCS also present additional basal ganglia atrophy compared to those without (Yang *et al.*, 2017), the basal ganglia may play an anticonvulsive role during seizures (Rektor *et al.*, 2012). A recent intracranial EEG study has reported changes in cortex–striatum synchronization level throughout focal seizures as a part of an endogenous mechanism controlling the duration and termination of abnormal oscillations (Aupy *et al.*, 2019). In some reports, the occurrence of dystonia, a semiology associated with increased basal ganglia activity (Cooper, 1962; Mizobuchi *et al.*, 2004), is negatively correlated with the presence of FBTCS in TLE (Cleto Dal-Cól *et al.*, 2008; Feddersen *et al.*, 2012; Popovic *et al.*, 2012; Uchida *et al.*, 2013). Specifically, Rektor *et al.* (2002, 2011) found the basal ganglia are only involved when the ictal activity has spread to other cortical areas, e.g. during secondary seizure generalization.

To date, the mechanisms implicated in such an inhibitory role for the basal ganglia remain largely hypothetical. In TLE, the basal ganglia–thalamocortical loops have been implicated in studies involving animal models (Vuong and Devergnas, 2018). Yet, *in vivo*, the organization of these circuits, and importantly the interaction between the basal ganglia and the thalamus, have rarely been studied, particularly with regard to FBTCS. Given that the thalamus has long been recognized as a seizure synchronizer (Guye *et al.*, 2006; Bertram *et al.*, 2008), we suspect that the presence of FBTCS may reflect a broken balance between basal ganglia inhibition and thalamic synchronization, which could reshape the interactions along the basal ganglia–thalamocortical loops.

To test this intuition, we used resting state functional MRI (rsfMRI) to assess the associations between the basal ganglia–thalamus–cortex interactions and the prevalence of FBTCS. Benefiting from the emerging computational tools and conceptual frameworks of network neuroscience (Bassett and Sporns, 2017), we evaluated the topological organization of these networks. First, using the participation coefficient, we assessed the degree to which the thalamus played the role of a connector hub in thalamocortical networks, enhancing its ability to facilitate communication among brain networks (Hwang *et al.*, 2017). We expected that greater hubness would promote cross-network communication for broader synchronization, such as that observed in secondary generalization. Second, using the interregional integration (Bassett *et al.*, 2015), we assessed the interactions within the basal ganglia–thalamus circuitry. We predicted that the occurrence of FBTCS would trigger the proposed basal ganglia inhibitory mechanism more excessively and eventually reshape the network's organization.

Importantly, both the basal ganglia and the thalamus are involved not only in FBTCS, but also in more restricted focal seizures (Blumenfeld *et al.*, 2004), and they contribute to the disruption of large-scale cortico-subcortical functional networks in focal epilepsies (Výtvarová *et al.*, 2017). To address the unique network characteristics associated with FBTCS, our main comparisons were made across three groups of TLE patients with distinct histories with respect to FBTCS (i.e. none, remote, and current). We hypothesized that the topological characteristics of thalamocortical and basal ganglia–thalamus networks may inform not only the presence but also the effective control of FBTCS.

Materials and methods

Participants

Ninety-six patients with refractory unilateral TLE were recruited from the Thomas Jefferson Comprehensive Epilepsy Center. Diagnosis was determined by a multimodal evaluation including neurological history and examination, interictal and ictal scalp video-EEG, MRI, PET, and neuropsychological testing (Sperling, 1996). As previously published, localization was determined after assessing that the testing was concordant for unilateral TLE. Patients were excluded from the study for any one of the following reasons: previous brain surgery, evidence of extra-temporal or multifocal epilepsy by history or testing, contraindications to MRI, or hospitalization for any Axis I disorder listed in the DSM-5 (Diagnostic and Statistical Manual of Mental Disorders, V). Depressive disorders were admissible given the high co-morbidity of depression and epilepsy (Tracy *et al.*, 2007).

All patients had focal impaired awareness seizures (FIAS) and/or FAS (focal aware seizures), and some had FBTCS as well. For the purpose of this study, patients were placed into one of three groups (32 participants each) based on their

history at the time of scanning: (i) patients who had never had any FBTCS events during their lifetime were assigned to the 'none-FBTCS' group; (ii) patients who had a remote history of FBTCS, but none for 1 year or more prior to scanning, were assigned to the 'remote-FBTCS' group; and (iii) patients who had recurrent FBTCS within 1 year prior to scanning were assigned to the 'current-FBTCS' group. To provide a neuroimaging reference, 32 demographically matched healthy control subjects were also recruited (Supplementary Table 3). All control subjects were free of psychiatric or neurological disorders based on health screening measures. This study was approved by the Institutional Review Board for Research with Human Subjects at Thomas Jefferson University. All participants provided informed consent in writing.

Imaging acquisition and preprocessing

Onsite MRI data, including T₁-weighted structural image and 5-min rsfMRI scan, were obtained from all participants. Details regarding MRI acquisition and data preprocessing, including mitigation of motion artefact with spike regression and scrubbing (Satterthwaite *et al.*, 2013), are described in the Supplementary material.

Functional parcellation of striatum and thalamus

We used a hybrid method to define regions of interest using both structural and functional information. Components of the basal ganglia were structurally defined with the 'atlas of the basal ganglia' (ATAG, <https://www.nitrc.org/projects/atag/>) (Keuken *et al.*, 2014), including the striatum, GPe and GPi, STN, and SN. We also localized the spatial extent of the thalamus based on the Morel atlas (Morel *et al.*, 1997; Krauth *et al.*, 2010). Because of the relatively small size of the GPi, GPe, STN and SN (Supplementary Table 1), these components were treated as regions of interest without any additional processing. For the striatum and thalamus, we then performed a masked independent component analysis (ICA)-based functional parcellation (Moher Alsady *et al.*, 2016) to divide them into functionally distinctive subdivisions. Although these structures could be further broken down with anatomical information, ICA provided specific functional dissociations between the subdivisions, which can be crucial for studying their functional interactions. To ensure that this functional parcellation remained neutral across all experimental groups, the procedure was performed on an independent set of preprocessed rsfMRI data from the Human Connectome Project (HCP) (<https://www.humanconnectome.org/>). Descriptions regarding this HCP dataset are provided in the Supplementary material.

Briefly, we masked the preprocessed HCP data with unilateral striatum and thalamus regions of interest and spatially smoothed the data with a 6-mm kernel. We then performed ICA to generate a functional parcellation by applying a 'winner-take-all' strategy (Moher Alsady *et al.*, 2016). To determine how many subdivisions were optimal for the unilateral striatum and thalamus, we ran the masked ICA across several dimensionalities for each mask using a split-half cross-validation strategy (Moher Alsady *et al.*, 2016). We found that a

dimensionality of 10 for bilateral striatum and a dimensionality of 7 for bilateral thalamus provided the best cross-validation stability (Supplementary Fig. 1). Accordingly, we parcelled each striatum into 10 subdivisions and each thalamus into seven subdivisions, which were generally symmetric in location and size (Fig. 1A).

Based on this hybrid method, 21 regions of interest were generated for each hemisphere (Supplementary Table 1). We then extracted the mean time series from the preprocessed onsite rsfMRI data using these subcortical regions of interest, as well as 200 cortical regions of interest defined in Schaefer *et al.* (2018). For the subsequent network analyses, these time series were used to generate Pearson correlation matrices within each hemisphere, separately, keeping in line with the unilateral nature of the basal ganglia–thalamocortical loops (Alexander *et al.*, 1986; Parent and Hazrati, 1995; Jones, 2007). We further removed the unreliable connections (e.g. correlations with an FDR-corrected P -value > 0.05) by setting their weights to zero, and took the absolute value of all remaining connection weights for all the matrices.

Distribution pattern of thalamocortical connections

To test our hypothesis that the thalamus plays a role as a connector hub in the brain to facilitate secondary generalization of seizures, we estimated the participation coefficient of each thalamic parcel to describe how uniformly the intrinsic functional connectivity between the thalamic and the cortical regions of interest were distributed across seven well-known cortical resting state networks (Yeo *et al.*, 2011) (Supplementary material and Fig. 1B). In a nutshell, a thalamic parcel with more uniformly distributed thalamocortical connections will present a participation coefficient closer to 1, and in contrast, one with more varying distributed connections will present a participation coefficient closer to 0.

Community detection-based interregional integration

To investigate the interaction between the basal ganglia and the thalamus, we applied a generalized Louvain-like community detection algorithm (Newman and Girvan, 2004; Reichardt and Bornholdt, 2006; Blondel *et al.*, 2008) on the functional connectivity matrix among the 21 subcortical basal ganglia and thalamic regions of interest, to identify groups of regions of interest with higher preference for interacting with each other (i.e. communities). This algorithm is described in the Supplementary material. We used interregional integration to represent the probability of all the regions of interest from two different partitions being assigned to the same community over iterative applications of the algorithm (Supplementary material). Intuitively, a higher value of integration represented a higher probability of the members from one partition being assigned to the same community with the members from another partition, potentially suggesting a higher functional interaction between these two anatomical structures (Fig. 1C).

For each basal ganglia–thalamus network, the 21 regions of interest were grouped following their main anatomical boundaries into five partitions: the striatum ($n = 10$), globus pallidus

($n = 2$), STN ($n = 1$), SN ($n = 1$), and thalamus ($n = 7$), yielding 10 pairwise integration values between every possible pair. Subsequently, the striatum was further broken down into caudate ($n = 4$), ventral striatum ($n = 1$), and putamen ($n = 5$), while the thalamus was further broken down into anterior ($n = 1$), medial-dorsal ($n = 1$), lateral-ventral ($n = 3$), and posterior ($n = 2$) nuclear groups (Krauth *et al.*, 2010) to finely probe pairwise functional interactions. Previously, we quantitatively demonstrated that the estimated integration value is independent of partition size (i.e. the number of regions of interest in a partition) (He *et al.*, 2018). Any such bias would be distributed uniformly across the groups, and hence would not affect our between-group comparisons.

To confirm that our results were relevant to the topological organization of the basal ganglia–thalamus network, we used a random network null model as a benchmark (Rubinov and Sporns, 2011), by testing whether interregional integration estimated from the null networks with random topological organization could produce results similar to those observed in real brain networks (Supplementary material).

Permutation-based statistical testing

To minimize the bias of data distribution to our statistical inferences and to correct for multiple comparisons, we implemented a permutation-based method as our main statistical strategy (Groppe *et al.*, 2011). Briefly, the observed statistic for each variable was compared to the distribution of the most extreme statistic across the entire family of tests for each possible permutation, thereby producing multiple comparison corrected P -values by controlling the family-wise error rate (Blair and Karniski, 1993) (Supplementary material). We performed 1 million permutations each time, and used either t - or F -statistics as appropriate.

As the hemispheric lateralization of the seizure focus may be irrelevant for FBTCs history in TLE patients (Bone *et al.*, 2012), the network properties of the right TLE patients were flipped left to right, allowing all statistical analyses to be conducted in accordance with the side of ictal onset (left, ipsilateral; right, contralateral). This method has been used previously to increase statistical power (Bernhardt *et al.*, 2010; He *et al.*, 2017; Yang *et al.*, 2017). Comparisons for common demographic and clinical information were made with standard parametric tests such as a one-way ANOVA or chi-square, conducted using IBM® SPSS® v25. The alpha level was set at $P < 0.05$ for both parametric and non-parametric tests.

Data availability

The data that support the findings of this study are available from the corresponding author upon reasonable request.

Results

Demographical, clinical and data quality

All three patient groups were matched by age, sex and handedness (Oldfield, 1971), as well as the lateralization

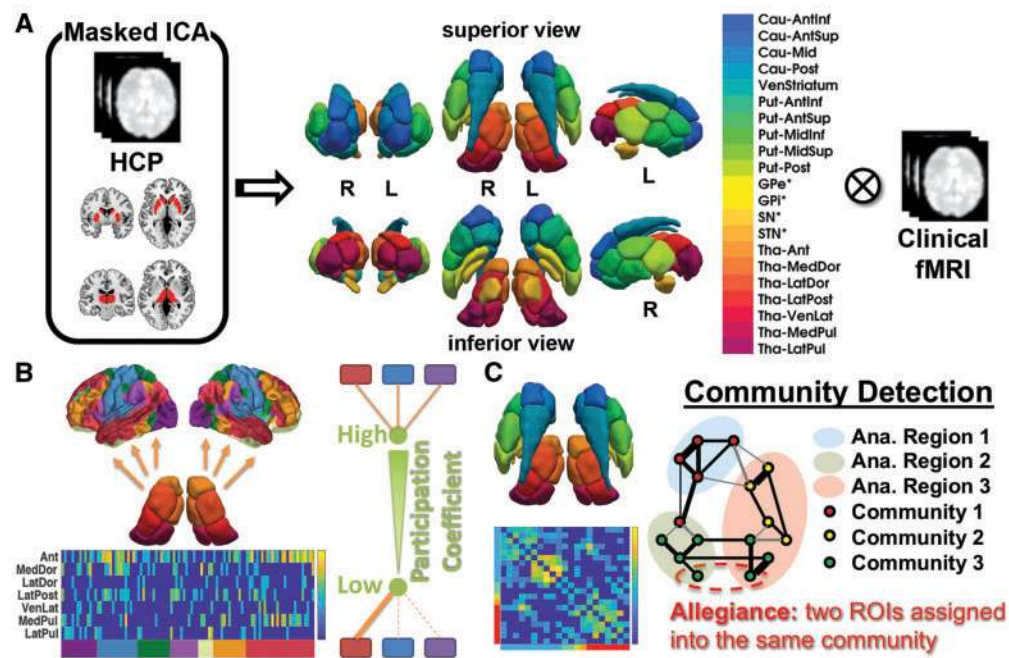


Figure 1 Schematic overview of the analytical pipeline. (A) We applied masked independent component analysis (ICA) (Moher Alsady *et al.*, 2016) on an independent rsfMRI dataset from the Human Connectome Project (HCP, $n = 100$) to generate functional parcellations of the striatum (10 parcels) and thalamus (seven parcels). In addition, anatomical masks for GPe and GPI, STN, and SN were directly adopted from the ATAG atlas (Keuken *et al.*, 2014), yielding a final parcellation scheme of the basal ganglia–thalamus network with 21 regions of interest (ROIs) per hemisphere. These regions of interest were then used to extract time series from the clinical rsfMRI data collected in this study. (B) Based on the Schaefer Atlas (Schaefer *et al.*, 2018), we estimated thalamocortical functional connectivity between each thalamic parcel and cortical regions of interest, and then sorted them by seven predefined resting state networks (Yeo *et al.*, 2011). We used the participation coefficient to represent the distribution pattern of thalamocortical functional connections across different resting state networks. The more uniform the distribution, the higher the participation coefficient, and vice versa. (C) We also estimated the functional connectivity matrix of the basal ganglia–thalamus network, on which we applied a community detection algorithm, to identify groups of regions of interest with higher preference for interacting with each other (i.e. communities) (Newman and Girvan, 2004; Reichardt and Bornholdt, 2006; Blondel *et al.*, 2008). We used interregional integration to represent the probability of all the regions of interest from two different anatomical origins being assigned to the same community (i.e. allegiance) over iterative applications of this algorithm (specifically, 1000 optimizations of a modularity quality index).

of their seizure focus (Table 1). As the presence of FIAS can also affect the basal ganglia and the thalamus (Blumenfeld *et al.*, 2004), we compared the frequency of FIAS among these patients, and found no significant differences. However, these patients did have differences in some other clinical features. Specifically, we noted the remote-FBTCS group showed earlier age at epilepsy onset, and longer disease duration compared to the other two groups. In addition, the none-FBTCS group had more varied temporal pathologies as evidenced by presurgical MRI scans. To test for group differences mainly driven by FBTCS history, the influence of these demographic and clinical variances needed to be minimized. Accordingly, we treated them as potential confounding factors and regressed them out. We further examined two main factors that may also bias the subsequent functional connectivity analyses, namely the anatomical structure where functional MRI signals were extracted and the data quality regarding head motion control and community detection. Although we did not observe any significant group

differences (Supplementary material and Supplementary Tables 2–4), we also sought to minimize their impact by confound regression.

In total, 12 potential confounding factors were identified, including age, sex, handedness, seizure focus side, FIAS frequency, age at epilepsy onset, epilepsy duration, MRI-evidenced temporal pathology, mean framewise displacement (Jenkinson, 2002), number of spikes scrubbed, network density, and total subcortical grey matter volumes. All confounding factors were regressed out from the network properties with a linear regression model, and the residuals were taken for subsequent statistical inferences.

Distribution pattern of thalamocortical connections

Consistent with previous work (Hwang *et al.*, 2017), we observed high participation coefficient values across all eight thalamic nuclear groups (four for each hemisphere) in all three patient groups. To explore group differences in

Table 1 Sample demographic and clinical characteristics

Characteristic	TLE group (n)			F/χ^2	P
	None-FBTCS (32)	Remote-FBTCS (32)	Current-FBTCS (32)		
Age	41.75 ± 12.77	41.66 ± 16.34	37.63 ± 11.52	0.946	0.392
Gender, male/female	14/18	16/16	17/15	0.584	0.745
Handedness, R/L/A	26/6/0	28/3/1	26/4/2	N.A.	0.577*
Seizure focus, LT/RT	18/14	18/14	13/19	2.084	0.353
Age at epilepsy onset	27.88 ± 16.22	17.56 ± 10.02	24.44 ± 11.38	5.367	0.006
Duration of epilepsy	13.88 ± 15.06	24.09 ± 18.04	13.19 ± 12.50	5.056	0.008
Frequency of FIAS, n/month	7.96 ± 9.80	6.75 ± 11.55	7.24 ± 18.74	0.061	0.941
Temporal pathology, NB/HS/other	3/14/15	10/16/6	12/11/9	10.487	0.033
Seizure type					
FIAS	17	0	0		
FIAS/FAS	15	0	0		
FIAS + FBTCS	0	19	17		
FAS + FBTCS	0	0	1		
FIAS/FAS + FBTCS	0	13	9		
FBTCS	0	0	5		
Current anti-epileptic drugs by category					
VGNC	16	19	16		
GABAa agonist	0	4	3		
SV2a receptor-mediated	12	13	11		
CRMP2 receptor-mediated	11	6	13		
Multi-action	6	8	3		
VGCC	2	6	5		

Continuous variables are presented as mean ± standard deviation. FAS = focal aware seizure; handedness is classified as: left-handed (L), right-handed (R), and ambidextrous (A); seizure focus was classified as: left temporal (LT) and right temporal (RT) focus; temporal pathology was diagnosed by neuroradiologists based on presurgical MRI scans as: normal brain MRI (NB), hippocampal sclerosis (HS), and other pathologies (Other), such as tumour, dysplasia, encephalocele, etc; VGNC = voltage-gated Na⁺ channel blockage, e.g. phenytoin, carbamazepine, oxcarbazepine, eslicarbazepine, lamotrigine and zonisamide (plus T-type Ca⁺⁺ channel blockage); GABAa agonist = e.g. clonazepam, clobazam, lorazepam, traxene; SV2a receptor-mediated = e.g. levetiracetam; CRMP2 receptor-mediated = e.g. lacosamide (plus VGNC blockage); multi-action = e.g. Na⁺ valproate (VGNC + GABAa agonist), topiramate (VGNC + GABAa agonist + AMPA/kianate receptor blockage + carbonic anhydrase inhibitor); VGCC = voltage-gated Ca⁺⁺ channel blockage, e.g. pregabalin, gabapentin. Multiple anti-epileptic drugs from the same category for one patient were counted only once. For continuous variables, one-way ANOVAs were conducted. For categorical variables, chi-square tests were conducted. Significant differences are highlighted in bold, and the contributors to the differences are highlighted in bold and italics. *Fisher's exact test performed instead, as >20% of cells had an expected count <5.

participation coefficient further, we regressed out the confound variables and compared the participation coefficients across patient groups with a permutation-based *F*-test. Because the thalamocortical connections were specifically tested here, the confound of total subcortical grey matter volume was replaced with thalamus volume.

After correction for multiple comparisons, a significant group difference was only found in the ipsilateral medial-dorsal nuclei [$F(2,93) = 8.202$, $P_{\text{corr}} = 0.003$], where the none-FBTCS group showed a lower participation coefficient compared to the other two groups (none < remote: $P_{\text{Bonferroni}} = 0.001$; none < current: $P_{\text{Bonferroni}} = 0.004$; Fig. 2A). This result could be reproduced without confound regression, with participation coefficients estimated from binary matrices, or when bilateral functional thalamocortical connections were also taken into account (Supplementary material).

To determine the atypicality in the participation coefficient patterns, we brought in a group of demographically-matched healthy control subjects to provide a neuroimaging baseline. The five clinical confounding factors were

excluded from this analysis because they did not apply to healthy controls. In addition, as there was no way to flip healthy controls' data to match the ipsilateral versus contralateral side in right TLE patients, we instead calculated the deviation score of participation coefficient

$$Z_{\text{pat}} = (PC_{\text{pat}} - \mu_{\text{con}}) / \sigma_{\text{con}} \quad (1)$$

where μ_{con} and σ_{con} were the mean and standard deviation of the same thalamic participation coefficient from the healthy controls, for each patient at each hemisphere, and we flipped the *Z*-score of right TLE afterwards. We used a permutation-based one-sample *t*-test to assess the *Z*-scores of the medial-dorsal nuclei, and found the none-FBTCS group presented *Z*-scores comparable to 0 [$t(31) = 0.892$, $P_{\text{corr}} = 0.758$], while the remote-FBTCS group [$t(31) = 5.814$, $P_{\text{corr}} = 1.6 \times 10^{-5}$] and current-FBTCS group [$t(31) = 4.061$, $P_{\text{corr}} = 0.001$] presented *Z*-scores significantly >0 (Fig. 2B). These findings suggest that the latter two groups had elevated participation coefficient values in comparison to healthy control subjects.

Interregional integration between basal ganglia and thalamus

To determine whether the interregional integration between the basal ganglia and the thalamus differed among patients with different FBTCS history, we applied the permutation-based F -test to compare the 20 pairwise integration measures (10 for each hemisphere) across the three patient groups, after regressing out all confound variables. After correction for multiple comparisons, significant group differences were found in the striatum–globus pallidus integration [$F(2,93) = 7.693$, $P_{\text{corr}} = 0.016$] and the globus pallidus–thalamus integration [$F(2,93) = 10.446$, $P_{\text{corr}} = 0.002$], both on the ipsilateral side. Specifically, the current-FBTCS group presented higher striatum–globus pallidus integration (current > none: $P_{\text{Bonferroni}} = 0.002$; current > remote: $P_{\text{Bonferroni}} = 0.004$) and lower globus pallidus–thalamus integration (current < none: $P_{\text{Bonferroni}} = 1.7 \times 10^{-4}$; current < remote: $P_{\text{Bonferroni}} = 0.001$), compared to the other two groups (Fig. 3A). Results remained significant when not regressing out confounding variables, as well as when using different resolution parameter values during community detection (Supplementary material), suggesting their robustness to variations in our analysis strategy.

A natural explanation for our findings is that such group differences in interregional integration simply reflect the differences in functional connectivity intensity between these region pairs. Therefore, similar to the manner in which we tested the integration, we tested the pairwise functional connectivity intensity over the aforementioned 20 possible combinations, but did not find any significant group differences [F 's(2,93) < 4.381, P_{corr} 's > 0.252; Fig. 3B]. Through linear regression, we found the FBTCS history difference could still explain a significant proportion of variance in interregional integration, even when the most relevant pairwise functional connectivity intensity estimates were included in the model (Supplementary material). Collectively, these results suggest that the group differences

in interregional integration cannot be simply explained by the pairwise functional connectivity intensity; instead, higher order topological differences are also responsible.

To evaluate the role of topological organization in the basal ganglia–thalamus network, we performed the same analysis on the integration estimated from randomly rewired networks with degree and strength distributions preserved. Again after regressing out confound variables, we found no significant group difference [F 's(2,93) < 4.395, P_{corr} 's > 0.210; Fig. 3C]. This result verified the contribution of topological organization to the aforementioned group differences in interregional integration.

In line with the previous sections, we further calculated the Z -scores of integration values to assess atypicality where significant differences emerged. We found the none- and remote-FBTCS groups presented Z -scores comparable to 0 [$t(31)$'s < 0.661, P_{corr} 's > 0.885], while the current-FBTCS group presented Z -scores significantly different from 0 [striatum–globus pallidus: $t(31) = 5.519$, $P_{\text{corr}} = 1.9 \times 10^{-5}$; globus pallidus–thalamus: $t(31) = -5.268$, $P_{\text{corr}} = 1.6 \times 10^{-5}$; Fig. 3D]. In other words, the none- and remote-FBTCS groups maintained a similar basal ganglia–thalamus network organization compared to that of healthy controls, while the recent-FBTCS group had specific reorganization that led to their unique striatum–globus pallidus–thalamus integration pattern.

Globus pallidus centred interregional integration

As noted, the globus pallidus was the key structure associated with the changes in the basal ganglia–thalamus interactions in the current-FBTCS group. Accordingly, we further subdivided the globus pallidus based on its anatomical boundaries into GPe and GPi segments, and explored their interregional integration with other components. Furthermore, we also broke the striatum down into caudate, ventral striatum and putamen, and the thalamus into

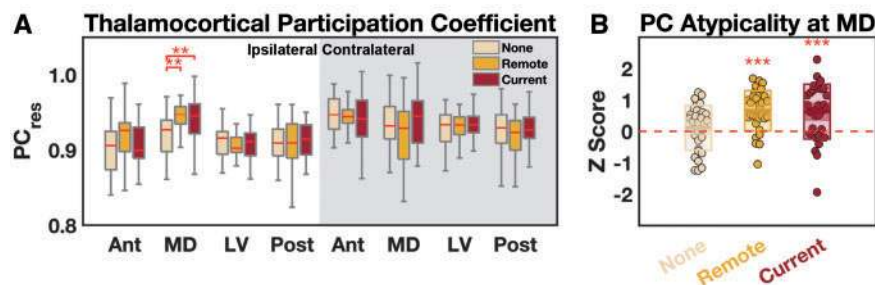


Figure 2 Thalamocortical participation coefficients compared across the three patient groups. (A) A significant difference was found in the ipsilateral medial-dorsal thalamic nuclear group. (B) Atypicality was estimated in reference to data obtained from a matched healthy control group. The remote- and current-FBTCS groups presented Z -scores significantly > 0, but not the none-FBTCS group. The full spectrum of Z -scores and data from healthy control group are presented in Supplementary Fig. 2. Ant = anterior; MD = medial-dorsal; LV = lateral-ventral; Post = posterior thalamic nuclear groups; res = residual after confound regression. ** $P < 0.01$; *** $P < 0.001$. Statistics were obtained via a non-parametric permutation test controlling for multiple comparisons. The central mark indicates the median, and the bottom and top edges of the box indicate the 25th and 75th percentiles, respectively.

anterior, medial-dorsal, lateral-ventral and posterior nuclear groups to provide a finer resolution assessment. Taking into consideration the STN and SN as well, we compared 18 (nine for each hemisphere) pairwise integration measures across the three patient groups for GPe and GPi, respectively, after regressing out confound variables.

Interestingly, after correction for multiple comparisons, no significant group differences could be found among the interregional integration estimates with the GPe [F 's(2,93) < 2.969, P_{corr} 's > 0.586; Fig. 4A]. In contrast, significant group differences were found in the putamen–GPi integration [F (2,93) = 9.926, P_{corr} = 0.003], the GPi–lateral-ventral nuclei integration [F (2,93) = 7.792, P_{corr} = 0.014], and the GPi–posterior nuclei integration [F (2,93) = 8.094, P_{corr} = 0.011], all on the ipsilateral side. Specifically, the current-FBTCS group presented higher putamen–GPi integration (current > none: $P_{\text{Bonferroni}}$ = 3.8×10^{-4} ; current > remote: $P_{\text{Bonferroni}}$ = 0.001), lower GPi–lateral-ventral nuclei integration (current < none: $P_{\text{Bonferroni}}$ = 0.001; current < remote: $P_{\text{Bonferroni}}$ = 0.008), and lower GPi–posterior nuclei integration (current < none: $P_{\text{Bonferroni}}$ = 0.028; current < remote: $P_{\text{Bonferroni}}$ = 4.6×10^{-4}), compared to the other two groups (Fig. 4B). Additionally, we observed negative correlations between the putamen–GPi integration and the two GPi–thalamus integration estimates (with lateral-ventral nuclei: R_{93} = -0.415, P = 2.9×10^{-5} ; with posterior nuclei: R_{93} = -0.427, P = 1.6×10^{-5}), even after controlling for the group index. The results were still robustly observed when we did not regress out confound variables (Supplementary material).

Again, we conducted the same Z -score analysis here to verify atypicality. We found that the none- and remote-FBTCS groups presented Z -scores comparable to 0 (t (31)'s < 0.955, P_{corr} 's > 0.718), while the current-FBTCS group presented Z -scores significantly different from 0 [putamen–GPi: t (31) = 4.544, P_{corr} = 1.6×10^{-4} ; GPi–lateral-ventral nuclei: t (31) = -5.227, P_{corr} = 5.4×10^{-5} ; GPi–posterior nuclei: t (31) = -4.486, P_{corr} = 5.3×10^{-4} ; Fig. 4C]. These results further confirmed that the current-FBTCS group displayed a specific increase in putamen–GPi integration and a decrease in GPi–thalamus integration mainly with the lateral-ventral and posterior nuclei, in reference to those of healthy control subjects.

Theoretically, the putamen can interact with the GPi through both direct and indirect pathways. Therefore, we sought to evaluate the influence of specific functional connectivities constituting each pathway on the observed interregional integration difference (Fig. 5A), by a simulated ‘disconnection’ method. First, we ‘disconnected’ the direct pathway by setting the functional connectivity values of all connections between putamen and GPi to 0, and reapplied the community detection and integration estimation. After regressing out the confound variables, no significant group differences were observed among pairwise integrations with either the GPe [F 's(2,93) < 2.344, P_{corr} 's > 0.798] or the GPi [F 's(2,93) < 3.864, P_{corr} 's > 0.331; Fig. 5B]. Specifically, if the caudate and ventral striatum (i.e. the

rest of the striatum) to GPi connections were zeroed out instead, the results were similar to the primary findings such that the three groups differed in pairwise integration of ipsilateral GPi [with putamen, F (2,93) = 9.072, P_{corr} = 0.005, Fig. 5C; with lateral-ventral nuclei, F (2,93) = 6.941, P_{corr} = 0.027; with posterior nuclei, F (2,93) = 7.369, P_{corr} = 0.019; others: F 's(2,93) < 3.974, P_{corr} 's > 0.299] but not GPe [F 's(2,93) < 3.544, P_{corr} 's > 0.407]. Second, we ‘disconnected’ the indirect pathway by zeroing out the functional connectivity values of all connections from putamen to GPe, GPe to STN, STN to GPi, and GPe to GPi, before applying community detection and estimating integration. After regressing out confound variables, we found group differences similar to the primary findings that involved pairwise integration of ipsilateral GPi [with putamen, F (2,93) = 12.730, P_{corr} = 3.2×10^{-4} , Fig. 5D; with lateral-ventral nuclei, F (2,93) = 6.271, P_{corr} = 0.049; with posterior nuclei, F (2,93) = 6.165, P_{corr} = 0.053; others: F 's(2,93) < 3.871, P_{corr} 's > 0.326] but not of GPe [F 's(2,93) < 5.149, P_{corr} 's > 0.111]. These results suggested that the functional connectivities emerging from the direct, but not the indirect, pathway contribute prominently to the observed GPi integration differences.

We further explored the GPi–thalamus integration differences (Fig. 6A) with a similar strategy. First, we ‘disconnected’ GPi and posterior thalamic nuclei by setting all their pairwise functional connectivity values to 0 before applying community detection and estimating integration. We found that this ‘disconnection’ simulation did not diminish the group differences in the ipsilateral GPi–thalamus integration [GPi–lateral-ventral nuclei: F (2,93) = 8.390, P_{corr} = 0.009; GPi–posterior nuclei: F (2,93) = 10.426, P_{corr} = 0.002; Fig. 6B]. Second, we ‘disconnected’ GPi and lateral-ventral thalamic nuclei before applying community detection and estimating integration. Although the GPi–posterior nuclei connections remained untouched, we no longer observed group differences in the ipsilateral GPi–thalamus integration [GPi–lateral-ventral nuclei: F (2,93) = 4.458, P_{corr} = 0.210; GPi–posterior nuclei: F (2,93) = 3.889, P_{corr} = 0.322; Fig. 6C]. Third, we ‘disconnected’ lateral-ventral and posterior thalamic nuclei instead. Interestingly this time, the group difference was only found in the ipsilateral GPi–lateral-ventral nuclei [F (2,93) = 9.317, P_{corr} = 0.004] but not in the GPi–posterior nuclei [F (2,93) = 1.944, P_{corr} = 0.922] integration (Fig. 6D). Collectively, these results suggest that the observed GPi–posterior nuclei integration differences may be prominently contributed by functional connectivities connecting GPi to lateral-ventral nuclei, and lateral-ventral to posterior nuclei.

Discussion

Pursuant to a network science perspective, we investigated the functional organization of the basal ganglia–thalamo-cortical loops in TLE patients with different FBTCS

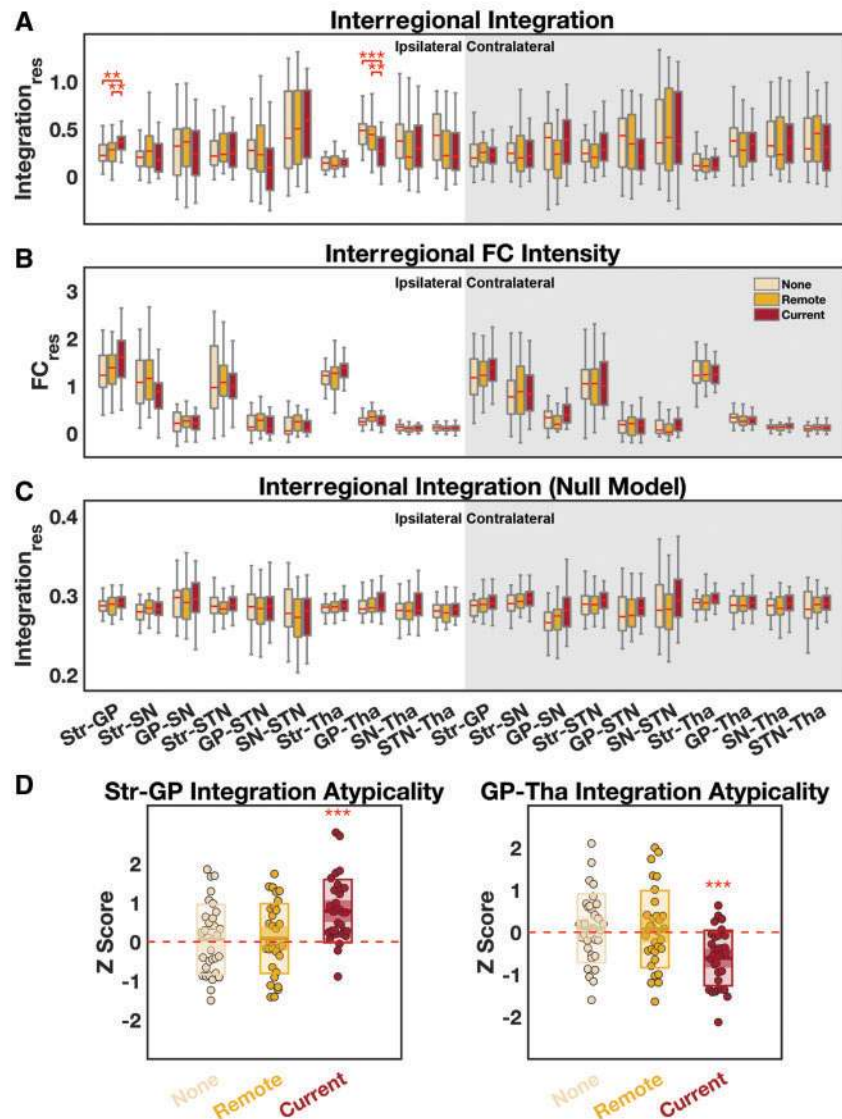


Figure 3 Pairwise interregional integration of the basal ganglia–thalamus network compared across the three patient groups.

(A) Significant differences in interregional integration were found at the striatum–globus pallidus (GP) and globus pallidus–thalamus pairs. (B) No significant differences were found when comparing pairwise functional connectivity instead of integration estimates. (C) No significant differences were found in a null model in which the original functional connectivity matrix was randomly rewired, preserving both the degree and strength distributions. (D) Atypicality was estimated in reference to data from a matched healthy control group. The current-FBTCS groups presented Z-scores significantly different from 0, but the other two groups did not. The full spectrum of Z-scores and data from the healthy control group are presented in Supplementary Fig. 3. FC = functional connectivity; res = residual after confound variable regression; Str = striatum; Tha = thalamus. $**P < 0.01$; $***P < 0.001$. Statistics were inferred with a non-parametric permutation-based method controlling for multiple comparisons. The central mark indicates the median, and the bottom and top edges of the box indicate the 25th and 75th percentiles, respectively.

histories. We found that, compared to patients who never experienced FBTCS, patients who had a positive history of FBTCS showed more uniformly distributed thalamocortical connections, particularly in the ipsilateral medial-dorsal thalamic nuclei. Patients with uncontrolled FBTCS also presented additional atypicalities in their basal ganglia–thalamus network compared to the other two patient groups, who were characterized by distinct putamen–GPi–thalamus interactions. These results suggest that the topological architecture of the thalamocortical network and

the basal ganglia–thalamus network together can inform both the presence and the effective control of FBTCS (Table 2).

The medial-dorsal nuclei are known to be connected to the hippocampus and other mesial temporal structures (Dolleman-Van der Weel *et al.*, 1997; Bertram and Zhang, 1999; Behrens *et al.*, 2003), and hence are heavily implicated in TLE. For instance, hypometabolism (Juhász *et al.*, 1999), structural abnormalities (Bernhardt *et al.*, 2012; Barron *et al.*, 2013), and altered thalamo-temporal

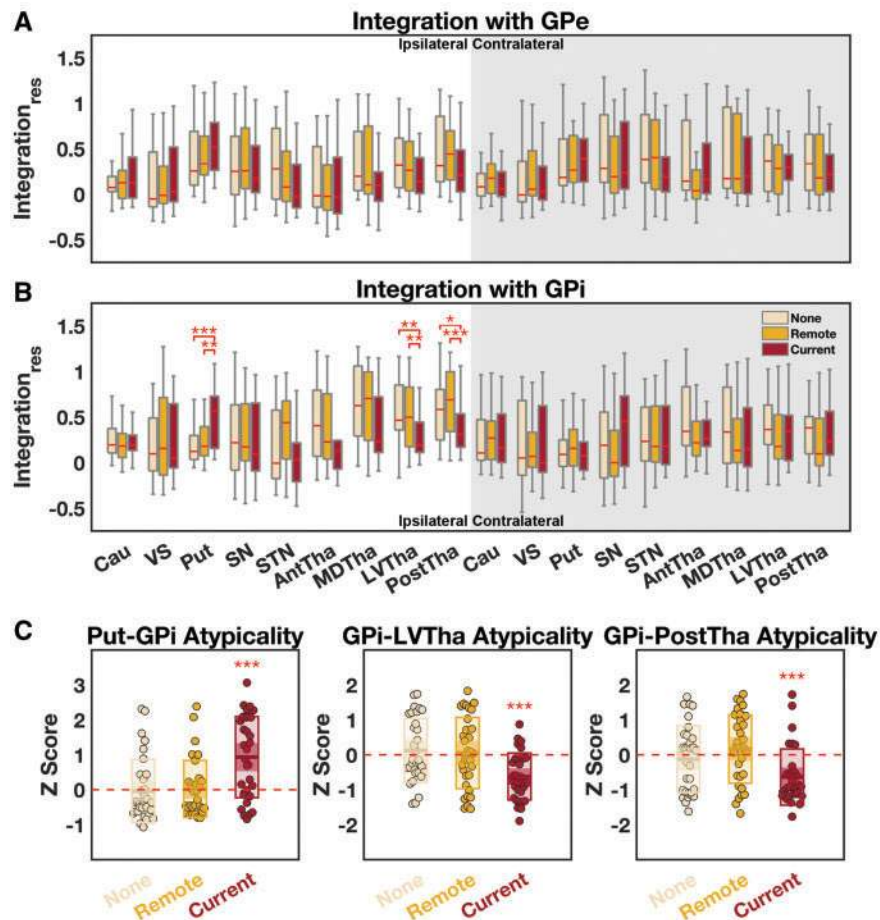


Figure 4 Interregional integration with GPe and GPi compared across three patient groups. **(A)** No significant differences were observed at the GPe. **(B)** Significant differences in interregional integration were observed in putamen–GPi, GPi–lateral-ventral thalamus, and GPi–posterior thalamus pairs. **(C)** Atypicality was estimated in reference to data from a matched healthy control group. The current-FBTCS groups presented Z-scores significantly different from 0, but the other two groups did not. The full spectrum of Z-scores and data from the healthy control group are presented in Supplementary Fig. 4. Ant = anterior; Cau = caudate; LV = lateral-ventral; MD = medial-dorsal; Post = posterior nuclear groups; Put = putamen; res = residual after confound variable regression; Tha = thalamus; VS = ventral striatum. * $P < 0.05$; ** $P < 0.01$; *** $P < 0.001$. Statistics were inferred with a non-parametric permutation-based method controlling for multiple comparisons. The central mark indicates the median, and the bottom and top edges of the box indicate the 25th and 75th percentiles, respectively.

connections (Keller *et al.*, 2014; He *et al.*, 2015) have been reported in the medial-dorsal nuclei of TLE patients. In particular, TLE patients with a history of FBTCS presented additional atrophy (Yang *et al.*, 2017) and disruption in thalamo-temporal connections (Keller *et al.*, 2015; Chen *et al.*, 2019) in the ipsilateral medial-dorsal nuclei than those without FBTCS. The medial-dorsal nuclei respond to the onset of limbic seizures (Bertram *et al.*, 2001; Blumenfeld *et al.*, 2007), and more importantly, facilitate seizure generalization (Bertram *et al.*, 2008). Increasing GABAergic inhibition to the medial-dorsal nuclei can suppress the response to stimulation-induced limbic seizures and further attenuate seizure propagation (Sloan *et al.*, 2011). Taken together, our finding of a greater integrating capacity in the ipsilateral medial-dorsal nuclei of the patients with positive FBTCS history is in line with these concepts. While causality cannot be implicated with cross-

sectional data, it is plausible that these effects are either a maladaptation to FBTCS, or are necessary to facilitate seizure spread that leads to FBTCS. Note that similar abnormalities were found in both the current- and the remote-FBTCS groups, suggesting that for the latter group, although their FBTCS were under control, they may still possess a vulnerability to FBTCS compared with patients who lack a history of FBTCS. Such shared functional abnormalities may in turn imply additional limbic neurophysiological alterations in these two groups. For instance, although we did not find any direct proof linking MRI-evidenced temporal pathology difference to the participation coefficient difference observed here (Supplementary material), the current- and the remote-FBTCS groups indeed included more cases of MRI-negative patients, who could still present with subtle limbic pathologies (Carne *et al.*, 2004).

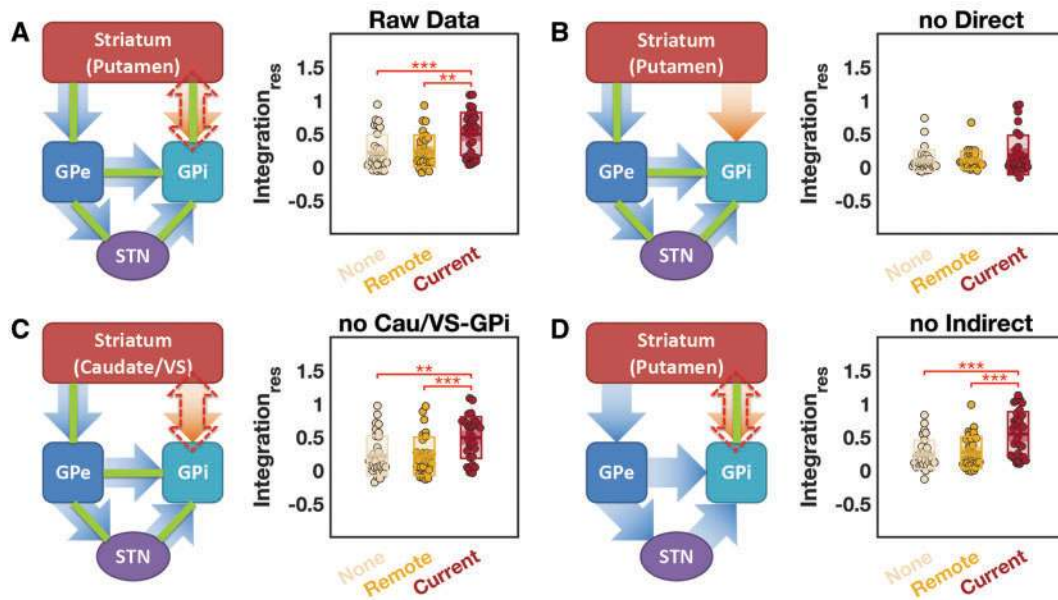


Figure 5 Simulated ‘disconnection’ analyses on putamen–GPI interregional integration. To delineate specific contributions from different connections of the network, we set functional connectivity value(s) of specific connection(s) to zero (i.e. ‘disconnected’), and then re-estimated the integration. **(A)** Before simulation, a significant group difference in putamen–GPI integration was found. **(B)** No significant putamen–GPI integration difference was found when the connections from putamen to GPI (i.e. the ‘direct pathway’) were ‘disconnected’. **(C)** A significant difference in the putamen–GPI integration was found when the connections from the caudate (Cau) and ventral striatum (VS) to the GPI were ‘disconnected’. **(D)** A significant difference in the putamen–GPI integration was found when all connections from putamen to GPe, GPe to STN, STN to GPI, and GPe to GPI (i.e. the ‘indirect pathway’) were ‘disconnected’. In the schematics, the orange arrow represents the direct pathway, the blue arrows represent both the long and short routes of the indirect pathway (Smith *et al.*, 1998), the green line represents functional connectivity, and the red dashed double head arrow represents the group difference in interregional integration. Bonferroni corrected *post hoc* test: ** $p < 0.01$; *** $p < 0.001$.

In addition to an altered thalamocortical network, our findings pointed to a reorganization in the basal ganglia–thalamus network specifically in patients with uncontrolled FBTCS, manifested as enhanced interactions between the putamen and the GPI, as well as reduced interactions between the GPI and the thalamus. In animal models, exogenous activation of the striatum protect against seizures (Cavalheiro *et al.*, 1987; Turski *et al.*, 1988; Sabatino *et al.*, 1989; Deransart *et al.*, 1998). In patients, endogenous hypersynchrony between the cortex and the striatum has been observed during seizure termination (Aupy *et al.*, 2019). It is proposed that the striatum modulates the basal ganglia output structures, such as the GPI and SN pars reticulata, thereby restoring thalamocortical synchrony and terminating the seizure (Aupy *et al.*, 2019). Although exactly when the striatum becomes involved remains controversial (Aupy *et al.*, 2019). Some scholars suggest the striatal response may be specifically associated with seizure spread and secondary generalization (Rektor *et al.*, 2002, 2011; Popovic *et al.*, 2012; Uchida *et al.*, 2013). Conceivably, this process in patients with uncontrolled FBTCS may be triggered more frequently, yielding a maladaptive increase in striatum–GPI integration.

Importantly, the striatum interacts with the GPI through both direct and indirect pathways, although their distinct

contributions to the proposed anticonvulsive process remain unclear (Vuong and Devergnas, 2018). Here, through a series of ‘disconnection’ simulations, we were able to articulate the importance of the direct pathway over the indirect pathway (Fig. 5) in revealing FBTCS-related changes in interregional integration. In the direct pathway, the striatum projects inhibitory GABAergic efferent connections directly to the GPI, which in turn provides tonic inhibition to the thalamus through GABAergic projections into the lateral and ventral thalamic nuclei (Lanciego *et al.*, 2012). Accordingly, one of the inherent products of an elevated putamen–GPI interaction would be GPI inhibition and, consequently, the reduction of its interaction with downstream targets, such as the lateral–ventral nuclei, matching the anti-correlations we observed between the two sets of integration estimates. In addition, GPI–posterior nuclei integration was also reduced in the current-FBTCS patients. Through our ‘disconnection’ simulations, we demonstrated that this difference largely depended upon functional connections from the GPI to the lateral–ventral nuclei, and from the latter to the posterior nuclei, but not upon the direct GPI–posterior nuclei connections (Fig. 6). Notably, these findings are tightly aligned with the physiological connections among these structures: the ventrolateral GPI receives input from the putamen and

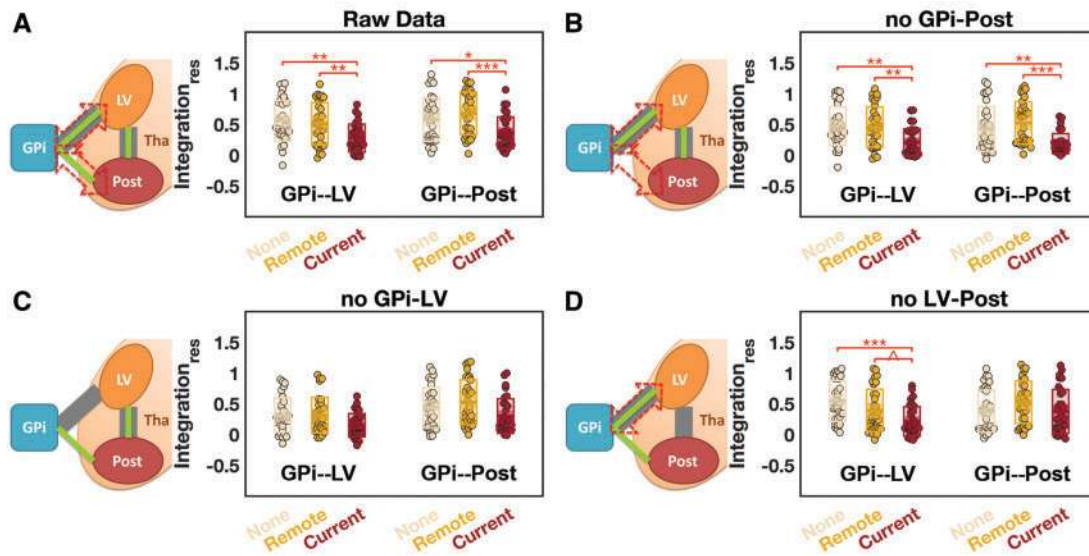


Figure 6 Simulated ‘disconnection’ analyses on GPI–thalamus interregional integrations. To delineate specific contributions from different connections of the network, we set functional connectivity value(s) of specific connection(s) to zero (i.e. ‘disconnected’), and then re-estimated the integration. **(A)** Before simulation, we observed significant group differences in GPI–lateral-ventral (LV) and in GPI–posterior (Post) thalamus integration. **(B)** Significant integration differences were still observed when the connections from GPI to the posterior thalamic nuclei were ‘disconnected’. **(C)** No significant integration differences were found when the connections from the GPI to the lateral-ventral thalamic nuclei were ‘disconnected’. **(D)** Significant integration differences were found at the GPI–lateral-ventral but not the GPI–posterior thalamus pair when all connections between the lateral-ventral and posterior thalamic nuclear groups were ‘disconnected’. In the schematics, thick grey lines represent anatomical connections, the green line represents functional connectivity, and the red dashed double headed arrow represents the group difference in interregional integration. Tha = thalamus. Bonferroni corrected *post hoc* test: $0.05 < ^*P < 0.1$; $*P < 0.05$; $**P < 0.01$; $***P < 0.001$.

Table 2 Schematic summary of findings

FBTCS history	Thalamus-mediated cortico-cortical communication	BG–thalamus interaction
None	Normative	Normative
Remote	Promoted	Normative
Current	Promoted	Reduced

BG = basal ganglia.

projects to the lateral-ventral thalamic nuclei, while the posterior thalamic nuclei do not receive direct projections from the GPI (Alexander *et al.*, 1986). Furthermore, ‘disconnecting’ the direct pathway removed group differences not only in the putamen–GPI integration, but also in both of the GPI–thalamus integrations. Accordingly, we suspect that these specific integration changes in the current-FBTCS patients may reflect one unified maladaptive reorganization process. Such a reorganization pattern was only observed in patients with uncontrolled FBTCS, potentially associated with the greater disease burden in this group (i.e. extra secondary seizure generalization). Alternatively, it may also imply that such reorganization is reversible, and can be restored once the FBTCS is under control.

Decreases in the GPI–thalamus interactions imply that in the current-FBTCS patients, the tonic thalamic inhibition from the GPI may be weakened. To our knowledge, there exists no direct evidence linking FBTCS with chronic disinhibition of the thalamus. Through single-unit

microelectrode recordings from anterior thalamic neurons, Hodaie *et al.* (2006) observed an atypical ‘hyperactive’ firing mode in awake patients with a history of generalized tonic-clonic seizures, which is consistent with our theory. In addition, FBTCS has been associated with greater reduction in the structural integrity of the thalamus (Yang *et al.*, 2017) and thalamocortical connections (He *et al.*, 2015; Keller *et al.*, 2015; Chen *et al.*, 2019), findings that may also be interpreted as the consequences of tonic pathological thalamic activity.

Among the anatomical thalamic nuclei included in our lateral-ventral and posterior regions of interest, the centromedian nuclei and medial pulvinar may be particularly relevant to FBTCS control in TLE, but probably through different roles. The medial pulvinar has reciprocal connections with both the medial and lateral part of the temporal lobe (Mauguiere and Baleyrier, 1978; Baleyrier and Mauguiere, 1985; Insausti *et al.*, 1987; Rosenberg *et al.*, 2009). During temporal lobe seizures, ictal involvement of

the medial pulvinar has been consistently recorded (Guye *et al.*, 2006; Rosenberg *et al.*, 2006). High-frequency stimulation (i.e. inhibition) of the medial pulvinar can reduce the severity of hippocampal seizures and shorten its generalization (Filipescu *et al.*, 2019). Therefore, a theoretical reduction in its tonic inhibition could lead to a higher susceptibility to seizure propagation from the temporal lobe (Rosenberg *et al.*, 2009). The centromedian nucleus is also considered a prominent target for brain stimulation in epilepsy, though more for its role in gatekeeping and rhythm-generating activities (Lega *et al.*, 2010). High-frequency stimulation of the centromedian nucleus was found mostly efficient in controlling primary and secondary generalized seizures (Velasco *et al.*, 1987, 2006; Fisher *et al.*, 1992). Accordingly, the theoretical reduction in its tonic inhibition could lead to a higher susceptibility to seizure generalization (Velasco *et al.*, 1989). Our findings imply that basal ganglia stimulation, such as GPi stimulation (Fisher and Velasco, 2014), may restore the tonic inhibition for all the downstream thalamic nuclei (Aupy *et al.*, 2019), leading to anti-epileptic effects in TLE patients with uncontrolled FBTCS.

Several methodological considerations are also pertinent to this study. First, due to the limited spatial resolution of rsfMRI, we did not further parcellate the SN into pars reticulata and pars compacta, acknowledging their distinct roles in the basal ganglia pathways. Second, the reliability of our findings depends heavily upon quality control during data processing. Therefore, we adopted the strategy proposed in Satterthwaite *et al.* (2013) using a combination of a sophisticated nuisance regression model and scrubbing. This strategy is sufficient for head motion control (Ciric *et al.*, 2017), even in studies based on short rsfMRI scans (Gu *et al.*, 2015; Xia *et al.*, 2018). However, it is also associated with lower degrees of freedom, which can harm statistical power during functional connectivity estimation (Parkes *et al.*, 2018). We also used linear regression to mitigate the effects of confounding factors including demographic, clinical, data quality, and brain structural variations among these patients. Nevertheless, we cannot fully rule out the existence of residual non-linear influences from these confounders, e.g. the underlying aetiology of epilepsy as expressed by differences in pathology among groups. Third, while our ‘disconnection’ simulation conveniently permits the comparison and contrast of different possible pathways, caution should be taken when interpreting these results, as functional connectivity essentially measures cross-regional couplings that can be attributed to both direct and indirect physiological connections. Accordingly, instead of mimicking an actual physical disconnection of specific anatomical tracts, this analysis probes putative functional interactions as a blueprint for brain stimulation. Fourth, our conceptual model omitted the connections between the basal ganglia and the prefrontal cortex, which is upstream of the basal ganglia pathways (Alexander *et al.*, 1986, 1990; Smith *et al.*, 1998). Whilst we made some efforts to test these connections (Supplementary material),

we did not find FBTCS-specific differences. Fifth, due to the lack of simultaneous EEG, we cannot completely rule out the existence of interictal activity during our scan, given its well-known and common effects in TLE (Laufs *et al.*, 2007). As functional connections, including thalamic and basal ganglia regions, have been shown to be very sensitive to interictal activity (Ibrahim *et al.*, 2014; Shamshiri *et al.*, 2017), the relationship between interictal activity and the functional organization of these networks warrants further investigation. Finally, we should note that some anti-epileptic drugs (AEDs) can influence the concentration of certain neurotransmitters such as GABA, hence potentially impacting the basal ganglia–thalamus interaction (Caciagli *et al.*, 2017). Unfortunately, AED regimen heterogeneity (type, dosage, number of AEDs) prevented further testing of these effects. Given the mixed distribution of AEDs across the patient groups (Supplementary Table 5), it seems unlikely that the observed difference could be traced to a specific medication.

In summary, we provide evidence that FBTCS imprint on the basal ganglia–thalamocortical loops in TLE patients. We demonstrate how a positive history of FBTCS relates to promoted thalamus-mediated cortico-cortical communication, and how uncontrolled FBTCS relates to reduced basal ganglia–thalamus interactions through the direct pathway. While future longitudinal studies may elaborate more on the underlying causality, our findings have brought additional clarity regarding specific links in the neural scaffolding underlying the presence of FBTCS. These mechanistic underpinnings may guide the development of new treatment strategies that may be used to either enhance or diminish interactions in specific circuits.

Acknowledgements

The authors thank Drs Gaelle Doucet and Dorian Pustina for help in data acquisition. We thank Drs Arian Ashourvan and Maxwell Bertolero for their suggestions. The authors thank all the healthy controls and patients with epilepsy, kept anonymous, who provided data for this study.

Funding

X.H. acknowledges grant support from the American Epilepsy Society. L.C. was funded by a ‘Berkeley Fellowship’ through UCL and Gonville and Caius College, Cambridge, and acknowledges previous support by Brain Research UK. D.S.B. acknowledges support from the John D. and Catherine T. MacArthur Foundation, the Alfred P. Sloan Foundation, the ISI Foundation, and NINDS R01-NS099348-01. J.I.T. acknowledges support from the NIMH R01-MH104606 and NINDS R01-NS112816-01. M.R.S. acknowledges support from the NIH and DARPA.

Competing interests

M.R.S. has research contracts through Thomas Jefferson University with UCB Pharma, Eisai, Medtronic, Takeda, SK Life Science, Neurelis, Engage Therapeutics, Xenon, and Cavion. He has consulted for Medtronic and NeurologyLive.

Supplementary material

Supplementary material is available at *Brain* online.

References

- Alexander GE, Crutcher MD, DeLong MR. Basal ganglia-thalamocortical circuits: parallel substrates for motor, oculomotor, 'prefrontal' and 'limbic' functions. *Prog Brain Res* 1990; 85: 119–46.
- Alexander GE, DeLong MR, Strick PL. Parallel organization of functionally segregated circuits linking basal ganglia and cortex. *Annu Rev Neurosci* 1986; 9: 357–81.
- Aupy J, Wendling F, Taylor K, Bulacio J, Gonzalez-Martinez J, Chauvel P. Cortico-striatal synchronization in human focal seizures. *Brain* 2019; 142: 1282–95.
- Baleydier C, Mauguier F. Anatomical evidence for medial pulvinar connections with the posterior cingulate cortex, the retrosplenial area, and the posterior parahippocampal gyrus in monkeys. *J Comp Neurol* 1985; 232: 219–28.
- Barron DS, Fox PM, Laird AR, Robinson JL, Fox PT. Thalamic medial dorsal nucleus atrophy in medial temporal lobe epilepsy: a VBM meta-analysis. *NeuroImage Clin* 2013; 2: 25–32.
- Bassett DS, Sporns O. Network neuroscience. *Nat Neurosci* 2017; 20: 353–64.
- Bassett DS, Yang M, Wymbs NF, Grafton ST. Learning-induced autonomy of sensorimotor systems. *Nat Neurosci* 2015; 18: 744–51.
- Behrens TEJ, Johansen-Berg H, Woolrich MW, Smith SM, Wheeler-Kingshott CAM, Boulby PA, et al. Non-invasive mapping of connections between human thalamus and cortex using diffusion imaging. *Nat Neurosci* 2003; 6: 750–7.
- Bernhardt BC, Bernasconi N, Concha L, Bernasconi A. Cortical thickness analysis in temporal lobe epilepsy: reproducibility and relation to outcome. *Neurology* 2010; 74: 1776–84.
- Bernhardt BC, Bernasconi N, Kim H, Bernasconi A. Mapping thalamocortical network pathology in temporal lobe epilepsy. *Neurology* 2012; 78: 129–36.
- Bertram EH, Mangan PS, Zhang D, Scott CA, Williamson JM. The midline thalamus: alterations and a potential role in limbic epilepsy. *Epilepsia* 2001; 42: 967–78.
- Bertram EH, Zhang DX. Thalamic excitation of hippocampal CA1 neurons: a comparison with the effects of CA3 stimulation. *Neuroscience* 1999; 92: 15–26.
- Bertram EH, Zhang DX, Williamson JM. Multiple roles of midline dorsal thalamic nuclei in induction and spread of limbic seizures. *Epilepsia* 2008; 49: 256–68.
- Blair RC, Karniski W. An alternative method for significance testing of waveform difference potentials. *Psychophysiology* 1993; 30: 518–24.
- Blondel VD, Guillaume J-L, Lambiotte R, Lefebvre E. Fast unfolding of communities in large networks. *J Stat Mech Theory Exp* 2008; 2008: P10008.
- Blumenfeld H. The thalamus and seizures. *Arch Neurol* 2002; 59: 135–7.
- Blumenfeld H, McNally KA, Vanderhill SD, Paige AL, Chung R, Davis K, et al. Positive and negative network correlations in temporal lobe epilepsy. *Cereb Cortex* 2004; 14: 892–902.
- Blumenfeld H, Rivera M, Vasquez JG, Shah A, Ismail D, Enev M, et al. Neocortical and thalamic spread of amygdala kindled seizures. *Epilepsia* 2007; 48: 254–62.
- Blumenfeld H, Varghese GI, Purcaro MJ, Motelow JE, Enev M, McNally KA, et al. Cortical and subcortical networks in human secondarily generalized tonic-clonic seizures. *Brain* 2009; 132: 999–1012.
- Blumenfeld H, Westerveld M, Ostroff RB, Vanderhill SD, Freeman J, Necochea A, et al. Selective frontal, parietal, and temporal networks in generalized seizures. *Neuroimage* 2003; 19: 1556–66.
- Bone B, Fogarasi A, Schulz R, Gyimesi C, Kalmar Z, Kovacs N, et al. Secondarily generalized seizures in temporal lobe epilepsy. *Epilepsia* 2012; 53: 817–24.
- Caciagli L, Xiao F, Wandschneider B, Koepp MJ. Imaging biomarkers of anti-epileptic drug action: insights from magnetic resonance imaging. *Curr Pharm Des* 2017; 23: 5727–39.
- Carne RP, O'Brien TJ, Kilpatrick CJ, MacGregor LR, Hicks RJ, Murphy MA, et al. MRI-negative PET-positive temporal lobe epilepsy: a distinct surgically remediable syndrome. *Brain* 2004; 127: 2276–85.
- Castro-Alamancos MA. Neocortical synchronized oscillations induced by thalamic disinhibition in vivo. *J Neurosci* 1999; 19: RC27.
- Cavaleiro EA, Bortolotto ZA, Turski L. Microinjections of the γ -aminobutyrate antagonist, bicuculline methiodide, into the caudate-putamen prevent amygdala-kindled seizures in rats. *Brain Res* 1987; 411: 370–2.
- Chen C, Li H, Ding F, Yang L, Huang P, Wang S, et al. Alterations in the hippocampal-thalamic pathway underlying secondarily generalized tonic-clonic seizures in mesial temporal lobe epilepsy: a diffusion tensor imaging study. *Epilepsia* 2019; 60: 121–30.
- Ciric R, Wolf DH, Power JD, Roalf DR, Baum GL, Ruparel K, et al. Benchmarking of participant-level confound regression strategies for the control of motion artifact in studies of functional connectivity. *Neuroimage* 2017; 154: 174–87.
- Cleto Dal-Cól ML, Berti P, Terra-Bustamante VC, Velasco TR, Araujo Rodrigues MC, Wichert-Ana L, et al. Is dystonic posturing during temporal lobe epileptic seizures the expression of an endogenous anticonvulsant system? *Epilepsy Behav* 2008; 12: 39–48.
- Cooper IS. Dystonia reversal by operation on basal ganglia. *Arch Neurol* 1962; 7: 132–45.
- Deransart C, Vercueil L, Marescaux C, Depaulis A. The role of basal ganglia in the control of generalized absence seizures. *Epilepsy Res* 1998; 32: 213–23.
- Dolleman-Van der Weel MJ, Lopes da Silva FH, Witter MP. Nucleus reuniens thalami modulates activity in hippocampal field CA1 through excitatory and inhibitory mechanisms. *J Neurosci* 1997; 17: 5640–50.
- Fedderson B, Remi J, Kilian M, Vercueil L, Deransart C, Depaulis A, et al. Is ictal dystonia associated with an inhibitory effect on seizure propagation in focal epilepsies? *Epilepsy Res* 2012; 99: 274–80.
- Filipescu C, Lagarde S, Lambert I, Pizzo F, Trébuchon A, McGonigal A, et al. The effect of medial pulvinar stimulation on temporal lobe seizures. *Epilepsia* 2019; 60: e25–30.
- Fisher RS, Uematsu S, Krauss GL, Cysyk BJ, McPherson R, Lesser RP, et al. Placebo-controlled pilot study of centromedian thalamic stimulation in treatment of intractable seizures. *Epilepsia* 1992; 33: 841–51.
- Fisher RS, Velasco AL. Electrical brain stimulation for epilepsy. *Nat Rev Neurol* 2014; 10: 261–70.
- Forsgren L, Bucht G, Eriksson S, Bergmark L. Incidence and clinical characterization of unprovoked seizures in adults: a prospective population-based study. *Epilepsia* 1996; 37: 224–9.
- Groppe DM, Urbach TP, Kutas M. Mass univariate analysis of event-related brain potentials/fields I: a critical tutorial review. *Psychophysiology* 2011; 48: 1711–25.

- Gu S, Satterthwaite TD, Medaglia JD, Yang M, Gur RE, Gur RC, et al. Emergence of system roles in normative neurodevelopment. *Proc Natl Acad Sci* 2015; 112: 13681–6.
- Guye M, Régis J, Tamura M, Wendling F, McGonigal A, Chauvel P, et al. The role of corticothalamic coupling in human temporal lobe epilepsy. *Brain* 2006; 129: 1917–28.
- Hamandi K, Salek-Haddadi A, Laufs H, Liston A, Friston K, Fish DR, et al. EEG-fMRI of idiopathic and secondarily generalized epilepsies. *Neuroimage* 2006; 31: 1700–10.
- Harden C, Tomson T, Gloss D, Buchhalter J, Cross JH, Donner E, et al. Practice guideline summary: Sudden unexpected death in epilepsy incidence rates and risk factors: report of the guideline development, dissemination, and implementation Subcommittee of the American Academy of Neurology and the American Epilepsy Society. *Neurology* 2017; 88: 1674–80.
- He X, Bassett DS, Chaitanya G, Sperling MR, Kozlowski L, Tracy JL. Disrupted dynamic network reconfiguration of the language system in temporal lobe epilepsy. *Brain* 2018; 141: 1375–89.
- He X, Doucet GE, Pustina D, Sperling MR, Sharan AD, Tracy JL. Presurgical thalamic “hubness” predicts surgical outcome in temporal lobe epilepsy. *Neurology* 2017; 88: 2285–93.
- He X, Doucet GE, Sperling M, Sharan A, Tracy JL. Reduced thalamocortical functional connectivity in temporal lobe epilepsy. *Epilepsia* 2015; 56: 1571–9.
- Hodaie M, Cordella R, Lozano AM, Wennberg R, Dostrovsky JO. Bursting activity of neurons in the human anterior thalamic nucleus. *Brain Res* 2006; 1115: 1–8.
- Holmes MD, Brown M, Tucker DM. Are ‘generalized’ seizures truly generalized? Evidence of localized mesial frontal and frontopolar discharges in absence. *Epilepsia* 2004; 45: 1568–79.
- Hwang K, Bertolero MA, Liu WB, D’Esposito M. The human thalamus is an integrative hub for functional brain networks. *J Neurosci* 2017; 37: 5594–607.
- Ibrahim GM, Cassel D, Morgan BR, Smith M Lou, Otsubo H, Ochi A, et al. Resilience of developing brain networks to interictal epileptiform discharges is associated with cognitive outcome. *Brain* 2014; 137: 2690–702.
- Insausti R, Amaral DG, Cowan WM. The entorhinal cortex of the monkey: III. Subcortical afferents. *J Comp Neurol* 1987; 264: 396–408.
- Jenkinson M. Improved optimization for the robust and accurate linear registration and motion correction of brain images. *Neuroimage* 2002; 17: 825–41.
- Jones EG. *The thalamus*. 2nd edn. Cambridge: Cambridge University Press; 2007.
- Juhász C, Nagy F, Watson C, da Silva EA, Muzik O, Chugani DC, et al. Glucose and [11C]flumazenil positron emission tomography abnormalities of thalamic nuclei in temporal lobe epilepsy. *Neurology* 1999; 53: 2037–45.
- Keller SS, O’Muircheartaigh J, Traynor C, Towgood K, Barker GJ, Richardson MP. Thalamotemporal impairment in temporal lobe epilepsy: a combined MRI analysis of structure, integrity, and connectivity. *Epilepsia* 2014; 55: 306–15.
- Keller SS, Richardson MP, Schoene-Bake JC, O’Muircheartaigh J, Elkommos S, Kreilkamp B, et al. Thalamotemporal alteration and postoperative seizures in temporal lobe epilepsy. *Ann Neurol* 2015; 77: 760–74.
- Keuken MC, Bazin P-L, Crown L, Hootsmans J, Laufer A, Müller-Axt C, et al. Quantifying inter-individual anatomical variability in the subcortex using 7 T structural MRI. *Neuroimage* 2014; 94: 40–6.
- Krauth A, Blanc R, Poveda A, Jeanmonod D, Morel A, Székely G. A mean three-dimensional atlas of the human thalamus: generation from multiple histological data. *Neuroimage* 2010; 49: 2053–62.
- Lanciego JL, Luquin N, Obeso JA. Functional neuroanatomy of the basal ganglia. *Cold Spring Harb Perspect Med* 2012; 2: a009621.
- Laufs H, Hamandi K, Salek-Haddadi A, Kleinschmidt AK, Duncan JS, Lemieux L. Temporal lobe interictal epileptic discharges affect cerebral activity in ‘default mode’ brain regions. *Hum Brain Mapp* 2007; 28: 1023–32.
- Lawn ND, Bamlet WR, Radhakrishnan K, O’Brien participation coefficient, So EL. Injuries due to seizures in persons with epilepsy: a population-based study. *Neurology* 2004; 63: 1565–70.
- Lega BC, Halpern CH, Jaggi JL, Baltuch GH. Deep brain stimulation in the treatment of refractory epilepsy: update on current data and future directions. *Neurobiol Dis* 2010; 38: 354–60.
- Mauguière F, Baleyrier C. Topographical organization of medial pulvinar neurons sending fibres to Brodman’s areas 7, 21 and 22 in the monkey. *Exp Brain Res* 1978; 31: 605–7.
- Mizobuchi M, Matsuda K, Inoue Y, Sako K, Sumi Y, Chitoku S, et al. Dystonic posturing associated with putaminal hyperperfusion depicted on subtraction SPECT. *Epilepsia* 2004; 45: 948–53.
- Moher Alsayd T, Blessing EM, Beissner F. MICA-A toolbox for masked independent component analysis of fMRI data. *Hum Brain Mapp* 2016; 37: 3544–56.
- Morel A, Magnin M, Jeanmonod D. Multiarchitectonic and stereotactic atlas of the human thalamus. *J Comp Neurol* 1997; 387: 588–630.
- Newman MEJ, Girvan M. Finding and evaluating community structure in networks. *Phys Rev E* 2004; 69: 026113.
- Norden AD, Blumenfeld H. The role of subcortical structures in human epilepsy. *Epilepsy Behav* 2002; 3: 219–31.
- Oldfield RC. The assessment and analysis of handedness: the Edinburgh inventory. *Neuropsychologia* 1971; 9: 97–113.
- Parent A, Hazrati L-N. Functional anatomy of the basal ganglia. I. The cortico-basal ganglia-thalamo-cortical loop. *Brain Res Rev* 1995; 20: 91–127.
- Parkes L, Fulcher B, Yücel M, Fornito A. An evaluation of the efficacy, reliability, and sensitivity of motion correction strategies for resting-state functional MRI. *Neuroimage* 2018; 171: 415–36.
- Peng S-J, Hsin Y-L. Altered structural and functional thalamocortical networks in secondarily generalized extratemporal lobe seizures. *NeuroImage Clin* 2017; 13: 55–61.
- Popovic L, Vojvodic N, Ristic AJ, Bascarevic V, Sokic D, Kostic VS. Ictal dystonia and secondary generalization in temporal lobe seizures: a video-EEG study. *Epilepsy Behav* 2012; 25: 501–4.
- Reichardt J, Bornholdt S. Statistical mechanics of community detection. *Phys Rev E* 2006; 74: 016110.
- Rektor I, Kuba R, Brázdil M. Interictal and ictal EEG activity in the basal ganglia: an SEEG study in patients with temporal lobe epilepsy. *Epilepsia* 2002; 43: 253–62.
- Rektor I, Kuba R, Brázdil M, Chrastina J. Do the basal ganglia inhibit seizure activity in temporal lobe epilepsy? *Epilepsy Behav* 2012; 25: 56–9.
- Rektor I, Kuba R, Brázdil M, Haláček J, Jurák P. Ictal and peri-ictal oscillations in the human basal ganglia in temporal lobe epilepsy. *Epilepsy Behav* 2011; 20: 512–7.
- Rosenberg DS, Mauguière F, Catenoux H, Faillenot I, Magnin M. Reciprocal thalamocortical connectivity of the medial pulvinar: a depth stimulation and evoked potential study in human brain. *Cereb Cortex* 2009; 19: 1462–73.
- Rosenberg DS, Mauguière F, Demarquay G, Ryvlin P, Isnard J, Fischer C, et al. Involvement of medial pulvinar thalamic nucleus in human temporal lobe seizures. *Epilepsia* 2006; 47: 98–107.
- Rubinov M, Sporns O. Weight-conserving characterization of complex functional brain networks. *Neuroimage* 2011; 56: 2068–79.
- Sabatino M, Gravante G, Ferraro G, Vella N, Grutta G La, Grutta V La. Striatonigral suppression of focal hippocampal epilepsy. *Neurosci Lett* 1989; 98: 285–90.
- Satterthwaite TD, Elliott MA, Gerraty RT, Ruparel K, Loughhead J, Calkins ME, et al. An improved framework for confound regression and filtering for control of motion artifact in the preprocessing of resting-state functional connectivity data. *Neuroimage* 2013; 64: 240–56.
- Schaefer A, Kong R, Gordon EM, Laumann TO, Zuo X-N, Holmes AJ, et al. Local-global parcellation of the human cerebral cortex

- from intrinsic functional connectivity MRI. *Cereb Cortex* 2018; 28: 3095–114.
- Schindler K, Leung H, Lehnertz K, Elger CE. How generalised are secondarily ‘generalised’ tonic-clonic seizures? *J Neurol Neurosurg Psychiatry* 2007; 78: 993–6.
- Shamshiri EA, Tierney TM, Centeno M, St Pier K, Pressler RM, Sharp DJ, et al. Interictal activity is an important contributor to abnormal intrinsic network connectivity in paediatric focal epilepsy. *Hum Brain Mapp* 2017; 38: 221–36.
- Sherman SM, Guillery RW. *Functional connections of cortical areas: a new view from the thalamus*. Cambridge: MIT Press; 2013.
- Sloan DM, Zhang D, Bertram EH. Increased GABAergic inhibition in the midline thalamus affects signaling and seizure spread in the hippocampus-prefrontal cortex pathway. *Epilepsia* 2011; 52: 523–30.
- Smith Y, Bevan MD, Shink E, Bolam JP. Microcircuitry of the direct and indirect pathways of the basal ganglia. *Neuroscience* 1998; 86: 353–87.
- Sperling MR. Temporal lobectomy for refractory epilepsy. *J Am Med Assoc* 1996; 276: 470–5.
- Tracy JL, Dechant V, Sperling MR, Cho R, Glosser D. The association of mood with quality of life ratings in epilepsy. *Neurology* 2007; 68: 1101–7.
- Turski L, Cavalheiro EA, Bortolotto ZA, Ikonomidou-Turski C, Kleinrok Z, Turski WA. Dopamine-sensitive anticonvulsant site in the rat striatum. *J Neurosci* 1988; 8: 4027–37.
- Uchida CGP, Barsottini OGP, Caboclo LOSF, de Araújo Filho GM, Centeno RS, Carrete H, et al. Does the patient’s hand hold the key to preventing secondary generalization in mesial temporal lobe epilepsy? *Epilepsy Res* 2013; 105: 125–32.
- Velasco AL, Velasco F, Jimenez F, Velasco M, Castro G, Carrillo-Ruiz JD, et al. Neuromodulation of the centromedian thalamic nuclei in the treatment of generalized seizures and the improvement of the quality of life in patients with Lennox–Gastaut syndrome. *Epilepsia* 2006; 47: 1203–12.
- Velasco F, Velasco M, Ogarrio C, Fanghanel G. Electrical stimulation of the centromedian thalamic nucleus in the treatment of convulsive seizures: a preliminary report. *Epilepsia* 1987; 28: 421–30.
- Velasco M, Velasco F, Velasco AL, Luján M, Mercado JV. Epileptiform EEG activities of the centromedian thalamic nuclei in patients with intractable partial motor, complex partial, and generalized seizures. *Epilepsia* 1989; 30: 295–306.
- Vuong J, Devergnas A. The role of the basal ganglia in the control of seizure. *J Neural Transm* 2018; 125: 531–45.
- Výtvarová E, Mareček R, Fousek J, Strýček O, Rektor I. Large-scale cortico-subcortical functional networks in focal epilepsies: the role of the basal ganglia. *NeuroImage Clin.* 2017; 14: 28–36.
- Walczak TS, Leppik IE, D’Amelio M, Rarick J, So E, Ahman P, et al. Incidence and risk factors in sudden unexpected death in epilepsy: a prospective cohort study. *Neurology* 2001; 56: 519–25.
- Wichmann T, DeLong MR. The basal ganglia. In: Kandel ER, Schwartz JH, Jessell TM, Siegelbaum SA, Hudspeth AJ, editors. *Principles of neural science*. New York: McGraw-Hill; 2012.
- Xia CH, Ma Z, Ciric R, Gu S, Betzel RF, Kaczkurkin AN, et al. Linked dimensions of psychopathology and connectivity in functional brain networks. *Nat Commun* 2018; 9: 3003.
- Yang L, Li H, Zhu L, Yu X, Jin B, Chen C, et al. Localized shape abnormalities in the thalamus and pallidum are associated with secondarily generalized seizures in mesial temporal lobe epilepsy. *Epilepsy Behav* 2017; 70: 259–64.
- Yeo BTT, Krienen FM, Sepulcre J, Sabuncu MR, Lashkari D, Hollinshead M, et al. The organization of the human cerebral cortex estimated by intrinsic functional connectivity. *J Neurophysiol* 2011; 106: 1125–65.
- Yoo JY, Farooque P, Chen WC, Youngblood MW, Zaveri HP, Gerrard JL, et al. Ictal spread of medial temporal lobe seizures with and without secondary generalization: an intracranial electroencephalography analysis. *Epilepsia* 2014; 55: 289–95.